GALCIT SM Report 87-19

POSTBUCKLING DELAMINATION OF A STIFFENED COMPOSITE PANEL USING FINITE ELEMENT METHODS

S. Natsiavas*, C.D. Babcock** and W.G. Knauss**

California Institute of Technology

Pasadena, California 91125

August, 1987

*Research Fellow in Mechanical Engineering and Aeronautics
**Professor of Aeronautics and Applied Mechanics

ABSTRACT

A combined numerical and experimental study is carried out for the postbuckling behavior of a stiffened composite panel. The panel is rectangular and is subjected to static in-plane compression on two opposite edges to the collapse level. Nonlinear - large deflection - plate theory is employed, together with an experimentally based failure criterion. It is found that the stiffened composite panel can exhibit significant postbuckling strength.

INTRODUCTION

An understanding of the behavior of composite structures is important since these structures are increasingly finding wide use in many Engineering fields. An area of special interest is the investigation of the failure mechanisms in multilayered composite panels subjected to in-plane compression. The available data in the literature indicate that composites may have considerable postbuckling strength, depending on ply thicknesses and orientation [1-3]. Ignorance of their response and failure mechanisms results in an excessively conservative design, which does not fully exploit all of the possible structural advantages.

The problem of the postbuckling behavior has been extensively studied for metal structures, but some new phenomena may arise for layered composite structures. For example, one of the most frequently observed failure in stiffened composites is debonding and separation of stiffeners as the structure is loaded into the postbuckling regime. This failure is caused by the step change in thickness induced by the attachment of the stiffeners to the panel. When the panel buckles, some joints may fail, which leads to separation of a stiffener from the panel. This separation results in loss of the postbuckling load carrying ability and hence lowers the ultimate strength of the structure.

In order to be able to construct safe and efficiently stiffened panels from composite materials, it is necessary to first understand the mechanics of the stiffener/panel separation process. This understanding requires examination of the postbuckling behavior of the panels, which involves large out-of-plane displacements relative to the panel thickness. This situation in

turn implies that the governing equations are nonlinear, which makes it virtually impossible to obtain closed form solutions. As a result, the most commonly employed analytical studies on the subject are limited to finite element or other energy type methods [1-8]. In some of these approaches [5-7] documented to date, the composite plate is assumed to be isotropic or orthotropic and the emphasis is placed in the panel deflections or stresses under idealized boundary conditions. The finite element analysis performed in reference [3] assumes the plate to be anisotropic but idealized boundary conditions. This approach does not allow interaction between the panel and the stiffener. Finally, a more sophisticated analysis is presented in [1], in which the panel is modeled as a plate while parts of the stiffener are modeled as beams and parts as plates. This modeling is more accurate in that when the stiffener is modeled as a beam, distortion is not considered, which may thus result in considerable inaccuracies, depending on the properties of the stiffener and the panel.

OBJECTIVE AND METHODOLOGY

As is clear from the foregoing discussion, the existing models for the behavior of stiffened composite panels are still in the development stage. By using the assumptions of plate theory, these analysis predict the resultant forces and moments, while the displacement and stress fields are expected to be valid sufficiently far away from the joints. On the other hand, failure of the structure is most likely to occur along the lines where the thickness changes abruptly. For example, a sharp discontinuity will lead to a singular stress field at a reentrant corner. The determination of this stress field will depend heavily on the degree of idealization by the model [9,10]. The analysis becomes even more complicated if one attempts to account for interlaminar stresses at free edges [11-13].

In an effort to overcome the complexities associated with the conversion of resultant forces and moments to the three-dimensional stress field near the step in thickness, a simplified approach is adopted here. In the absence of a suitable failure criterion for the delamination of stiffened composite panels, the prediction of their ultimate strength is unavoidably dependent on experimental data. For a given panel stiffener construction and configuration, the relation

between the macro stresses (resultant forces and moments) and the micro stresses near the thickness discontinuity will be the same. Therefore, the failure condition for a fixed panel/stiffener intersection may be characterized in terms of resultant forces [14].

The objective is to first establish a failure envelope of the resultant forces, by performing experiments with the panel. Having this envelope, one will then have to determine analytically the levels of the applied loads which result in a critical combination of the resultant forces near the joints. Of course, such an envelope will depend on the properties, combination and orientation of the constituent laminae, as well as the configuration of the joints. However, this envelope will be the same for various stiffener spacings, provided that this spacing is long enough for the natural diffusion of the resultant forces to micro stresses to occur.

EXPERIMENT

Test Specimen

Determination of the failure envelope can be achieved by testing only a part of the whole panel. The specimen tested in this investigation was supplied by staff at NASA Langley and its dimensions are shown in Figure 1. The panel was constructed from 16 layers with orientation $[\pm 45/90/0]_{2S}$. Each lamina has a thickness of about 0.14 mm and behaves as an orthotropic material with the following properties

$E_1 = 13.1*10^{10}$ Pa, $E_2 = 1.3*10^{10}$ Pa

$G_{12} = 0.64*10^{10}$ Pa, $\nu_{12} = 0.38$

The stiffener was constructed from 8 additional layers of the same material, with orientation $[\pm 45]_4$. As shown in Figure 1, the stiffener occupies the area (ACHJ).

During testing, the edges AE and FJ were clamped on an aluminum frame, while the support provided along BI and DC simulated simply-supported conditions. The panel was loaded by applying compression on the edges AE and FJ, as explained next.

Test Setup

A 300 Klb - capacity hydraulic testing machine was used to apply the compressive loading on the specimen. The specimen was placed between the flat plates in the testing machine and adjusted for vertical alignment. Loading was applied in a displacement controlled fashion. In-plane and out-of-plane displacements at selected locations were monitored during the course of the experiment. Dial gauges resolving 10^{-4} inches and LVDT's were used for measuring these displacements. A load cell mounted in series with the specimen between the flat plates in the loading machine measured the load applied. The load displacement response was recorded until the specimen failed in the post-buckled region.

ANALYSIS

A finite element model was developed for the pre- and postbuckling calculations of the test specimen described in the previous section. The MSC/NASTRAN computer code was employed by utilizing the mesh shown in Figure 2. Both the unstiffened and the stiffened parts of the composite were modeled using plate elements. Each of the 210 rectangles in Figure 2 represents a 4-node quadrilateral anisotropic plate element (CQUAD4). Each node of these elements has five degrees-of-freedom, including the three displacements (u,v,w) and two rotations ($\partial w/\partial x$ and $\partial w/\partial y$). Both membrane and bending effects are thus considered, with the transverse shear being neglected. The 8-node elements would have been more appropriate for this type of problem, but they are not available in NASTRAN for calculations involving geometrical nonlinearity [15].

The stiffness matrix for each element is computed by the code, taking into account the orientation and the material properties of each individual lamina and using the assumptions of classical laminate plate theory. The boundary conditions were chosen to simulate as closely as possible the experimental conditions and they were as follows:

On AE: $u = v = w = \partial w/\partial x = \partial w/\partial y = 0$

On FJ: $u = \partial w/\partial x = \partial w/\partial y = 0, \quad N_y = -N = \text{constant}$

On BI,DG: $w = \partial w/\partial y = 0.$

With these boundary conditions, the total number of degrees-of-freedom for the mesh considered is 1020. In the calculations, the uniform compressive force applied on FJ was increased gradually and with relatively large increments before buckling. An estimate for the buckling load was obtained before the finite element analysis was run, by using the average material properties of the composite and assuming isotropic constitutive behavior. After buckling, the compressive load was increased in increments of about 5% of the buckling load. The analysis was carried out until the compressive load reached the failure value, as determined by the experiment.

RESULTS

Figure 3a depicts contours of constant out-of-plane displacement w, obtained by the finite element analysis for the experimentally determined critical in-plane load. Clearly, the part of the panel between the supports buckles in a half-wave pattern in both directions, which is in agreement with the observed displacement pattern during the experiment. The maximum out-of-plane displacement occurs near the center of the structure and is computed to be 4.54 mm, which is about two times the thickness of the panel. To examine the spatial convergence of the developed finite element mesh, other meshes were also used. Figure 3b, represents the displacement pattern which was obtained for the same structure and boundary conditions but from a coarser mesh (120 elements, 575 dof).

Figure 4a shows the pattern of the in-plane deformation of the structure, computed at the critical in-plane load. To make the pattern look clearer, the displacements in that graph are multiplied by a factor of 50. Similar results are shown in Figure 4b. These results were obtained from the coarse mesh discussed above. The in-plane displacements are smaller in the middle of the panel due to the large out-of-plane displacement in that area.

The relation between the total compressive end load and the corresponding average end-shortening is shown in Figure 5. The continuous line represents numerical results obtained by the finer finite element model, while the broken line corresponds to results from the coarse mesh. The stars represent experimental results in which the end-shortening is measured by a dial-

gauge, while the dots are experimental results where the inplane displacement is measured by the LVDT. Similar meaning is also given to the continuous, and broken lines and the stars on Figure 6. In this figure the displacement axis represents values of the out-of-plane displacement measured during the experiment, in the middle point of the panel. From both of these two graphs, it is observed that the numerically obtained curves show the same qualitative behavior as the experimental curves. This behavior is typical for the postbuckling behavior of plates and was also observed in previous work on the subject [1,2,5,7]. Also, both the experimental and the analytical results indicate that the panel exhibits substantial postbuckling strength. According to the experimental results appearing in Figures 5 and 6, the failure load is estimated to be about three times the buckling load of the structure.

Comparing the numerical with the experimental results, a considerable difference is observed. Some of that difference is expected and is probably due to the following reasons. First, the panel is modeled without taking into account geometrical imperfections. Also, the analytical boundary conditions do not match exactly the experimental support conditions, especially along the simply-supported edges and at the edge were the load is applied. From Figure 4 one can see clearly that by applying uniform forces along the edge, the in-plane displacement v of the loaded end is not uniform. Another factor that can affect the results is the accuracy of the values of the material properties, dimensions and orientations of the laminae. For example, the measured thickness of the panel was found to be about 10% less than the value obtained by multiplying the number of laminae of the composite times the thickness of each lamina. Finally, some of the numerical problems encountered by using the finite element code are discussed next.

By comparing the continuous with the broken lines of Figures 5 and 6, it is seen that the spatial convergence of the finite element mode is acceptable as far as the end-shortening and the out-of-plane displacement at the middle of the panel is concerned. Similar conclusions can be drawn by comparing Figures 3a and 4a with Figures 3b and 4b respectively. However, this is not the case when the contours of the resultant moments and forces are examined. Figure 7a depicts

contours of constant resultant shear force Q_x, obtained by the fine mesh at the critical load, while Figure 7b shows similar results obtained from the coarse mesh. Clearly, the convergence of this resultant load (which involves third derivatives of the out-of-plane displacement with respect to the spatial coordinates) is not satisfactory. A similar behavior was observed for the other resultant forces and moments. This indicates the need for more study on the subject. Finer meshes should be tried and at least another finite element code should be employed for the same problem and the obtained results should be compared with the present ones before any confidence in the numerical results is established. It is of great importance to investigate if and how the spatial convergence of the solution is affected by the presence of the step in thickness, induced by the stiffener [16]. Another area which needs further study is how the sudden stiffness reduction occurring at buckling, effects the convergence of the numerical solution. Clearly, the convergence of the resultant forces and moments is of vital importance since these loads are required in developing the proposed failure envelope for the structure.

Finally, for the composite panel tested, the resulting failure was due to delamination near the points G and I rather than the expected panel/stiffener separation. During the test, the panel deformed in such a way that the area near the step in thickness was under compression, rather than tension. As can be deduced from Figure 6, the maximum out-of-plane displacement for compressive loads near the failure level was about three times the thickness of the panel. This fact allowed the deformation pattern of the panel to be readily observable in the postbuckling regime.

SUMMARY AND CONCLUSIONS

A finite element model was developed for the postbuckling behavior of a stiffened graphite/epoxy rectangular plate loaded by in-plane compression. Both the unstiffened and the stiffened parts of the structure were modeled as anisotropic plates and the NASTRAN computer code was used for the numerical calculations. Experimental data for the same structure were also obtained and compared with the numerical results. The discrepancy between the numerical and the experimental results needs to be investigated further. Effects due to the change in

thickness induced by the stiffener and the great reduction of stiffness at buckling on the convergence of the numerical solution have yet to be examined. Resultant forces and moments need to be computed accurately if a failure envelope is to be established for a composite structure. Finally, both the numerical and the experimental results show that the stiffened panel can exhibit a significant postbuckling strength. From the experimental data, the failure load was about three times higher than the buckling load, indicating how much the design of such structures can be improved, once their behavior is reasonably predictable.

ACKNOWLEDGEMENTS

This work was supported by NASA, under grant number NSG 1483. The first author wishes to thank Professors C.D. Babcock and W.G. Knauss for the opportunity to work on this project and for many fruitful discussions. The help of Drs. J.F. Hall, G. Ravichandran and Mr. R. Madhaven is also gratefully acknowledged.

REFERENCES

1. Starnes, J.H., Knight, N.F. and Rouse, M., "Postbuckling Behavior of Selected Flat Stiffened Graphite-Epoxy Panels Loaded in Compression," AIAA Journal, Vol. 23, No. 8, pp. 1236-1246, 1985.

2. Stevens, K.A. and Davies, G.A., "Failure of Buckled Composite Plates," Intern. Symposium on Composite Materials and Structures," pp. 345-350, Beijing, China, June 1986.

3. Agarwal, B.L., "Postbuckling Behavior of Composite Shear Webs," AIAA Journal, Vol. 19, No. 7, July 1981, pp. 933-939.

4. Agarwal, B.L., "A Model to Simulate Failure Due to Stiffener/Web Separation of Composite Tension Field Panels," AIAA Paper No. 82-0746.

5. Stein, M., "Postbuckling of Orthotropic Composite Plates Loaded in Compression," AIAA Journal, Vol. 21, No. 12, Dec. 1983, pp. 1729-1735.

6. Stein, M., "Analytical Results for Postbuckling Behavior of Plates in Compression and in Shear," NASA TM 85766, March 1984.

7. Harris, G.Z., "Buckling and Postbuckling of Orthotropic Laminated Plates," AIAA Paper No. 75-813, 16th Structures, Structural Dynamics and Materials Conference, Denver, CO, 1975.

8. Turvey, G.J. and Wittrick, W.H. "The Large Deflection and Post-Buckling Behavior of Some Laminated Plates," Aeronautical Quarterly, Vol. 24, 1973, pp. 77-86.

9. Kuo, M.C. and Bogy, D.B., "Plane Solutions for the Displacement and Traction-Displacement Problems for Anisotropic Elastic Wedges," J. Applied Mechanics, March 1974, pp. 197-208.

10. Ting, T.C.T. and Chou, S.C., "Edge Singularities in Anisotropic Composites," Int. J. Solids Structures, Vol. 17, No. 11, pp. 1057-1068, 1981.

11. Pipes, R.B. and Pagano, N.J. "Interlaminar Stresses in Composite Laminates Under Uniform Axial Extension," J. Composite Materials, Vol. 4, 1970, pp. 538-550.

12. Wang, S.S. and Choi, I., "Boundary-Layer Effects in Composite Laminates," J. Applied Mechanics, Vol. 49, Sept. 1982, pp. 541-560.

13. Zwiers, R.I., Ting, T.C.T. and Spilker, R.L., "On the Logarithmic Singularity of Free-Edge Stress in Laminated Composites Under Uniform Extension," J. Applied Mechanics, Vol. 49, Sept. 1982, pp. 561-569.

14. Babcock, C.D. and Knauss, W.G., "Effect of Stress Concentration in Composite Structures," SM Report 84-17, Caltech, Pasadena, CA, 1984.

15. McCormick, W.C., (ed.), "MSC/NASTRAN User's Manual," MacNeal-Schwendler Corp., Los Angeles, CA.

16. Tong, P. and Pian, H.H., "On the Convergence of the Finite Element Method for Problems with Singularity," Int. J. Solids Structures, 1973, Vol. 9, pp. 313-321.

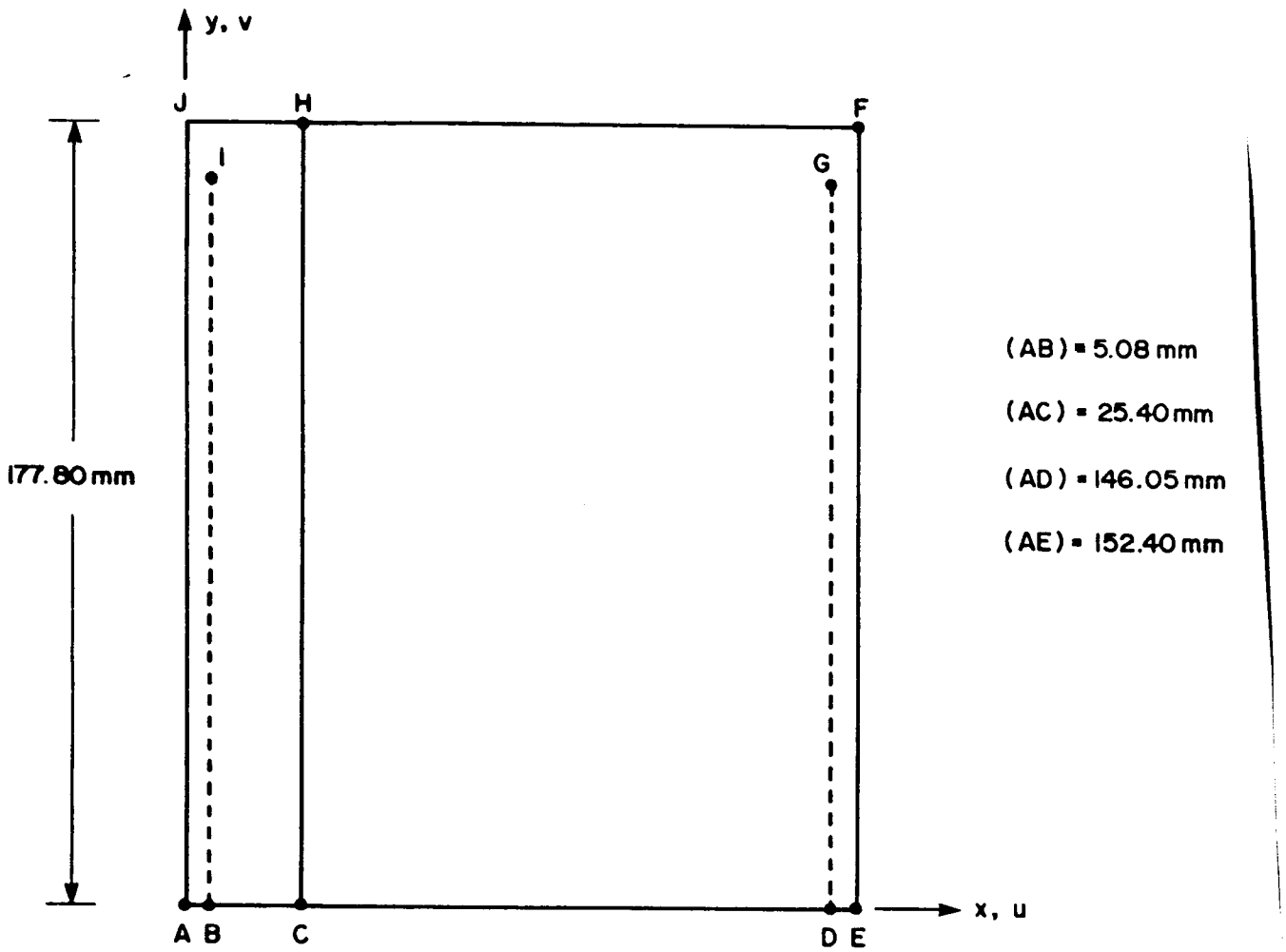

Figure 1. Specimen Geometry

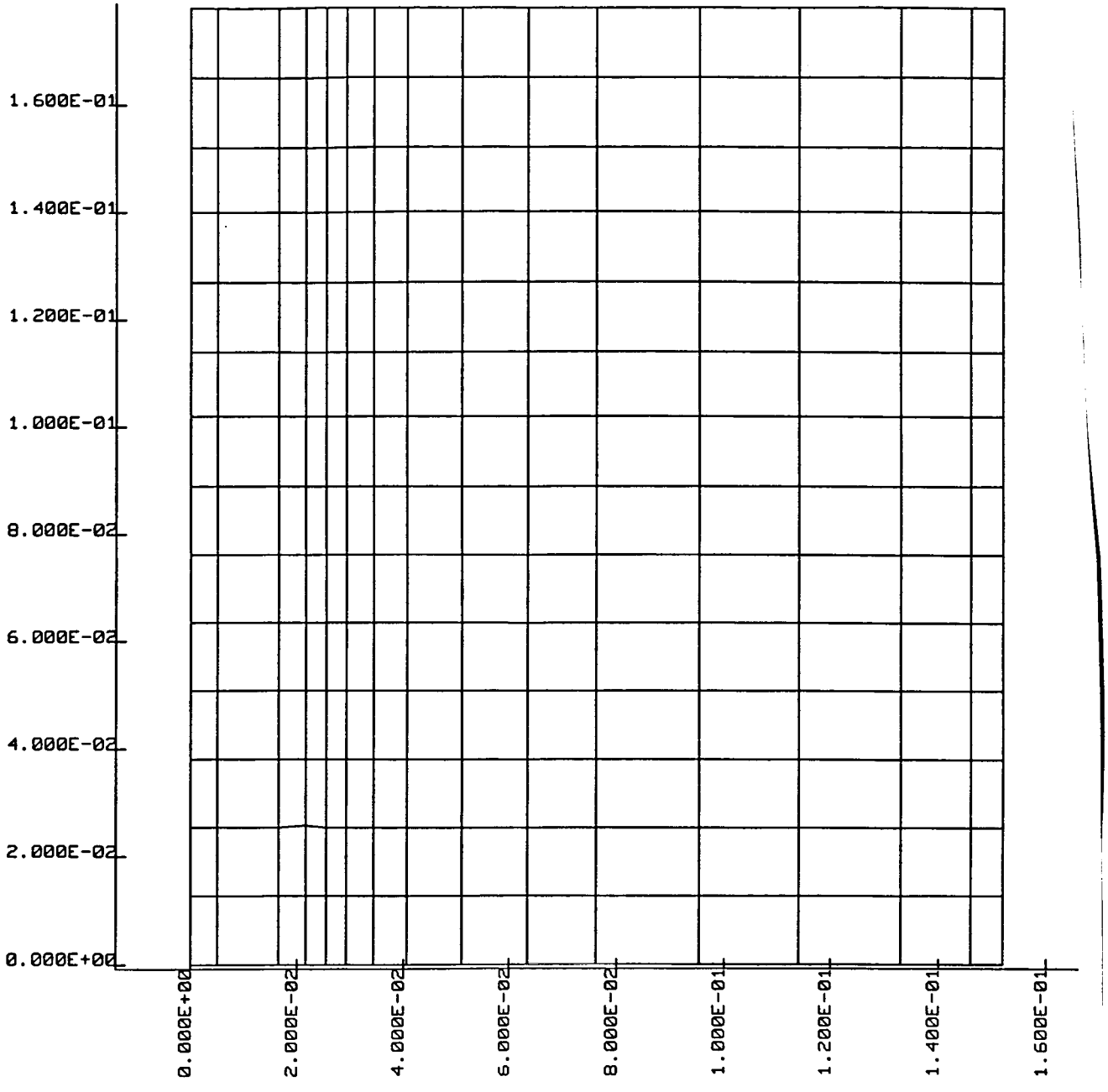

Figure 2. Finite Element Mesh

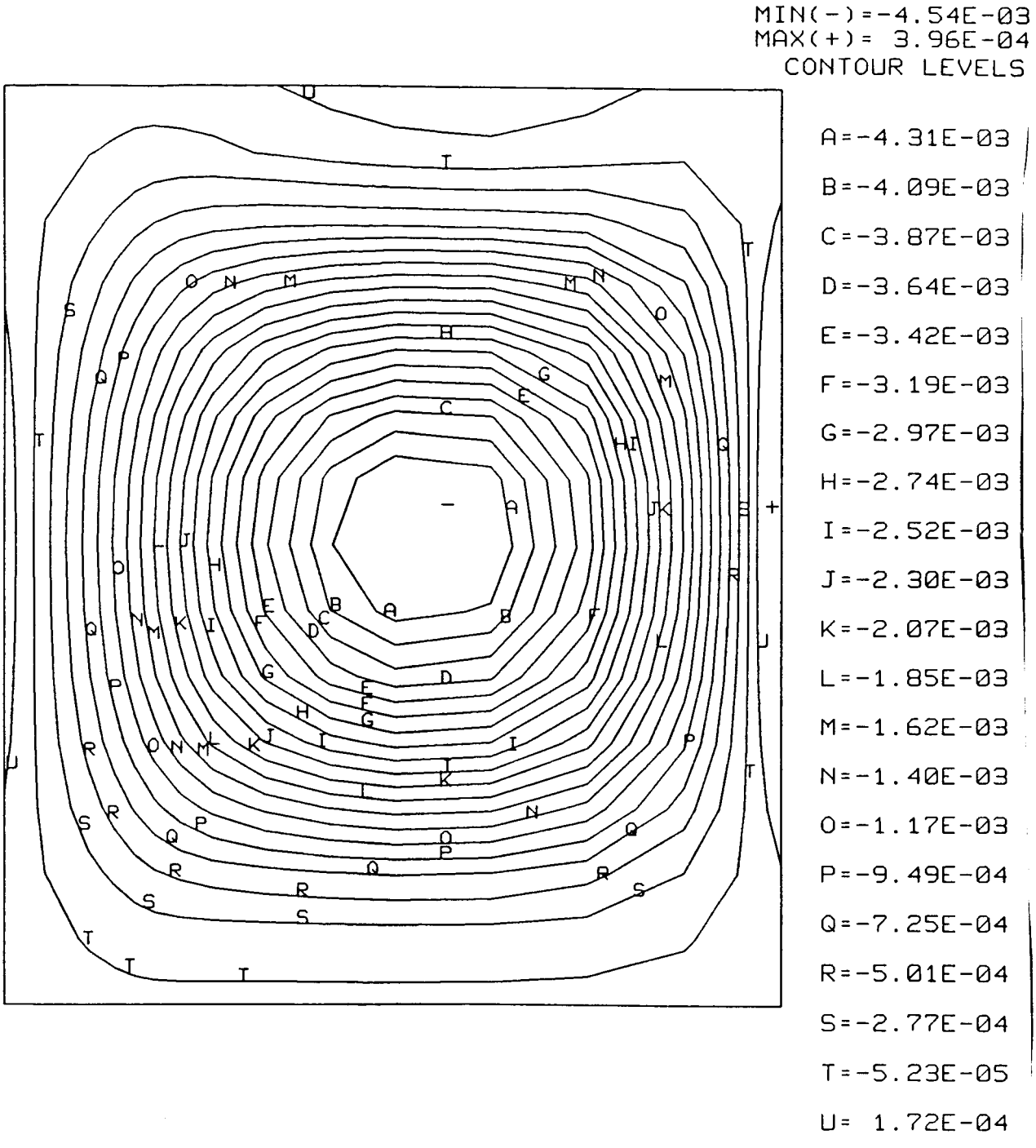

Figure 3a. Contours of constant out-of-plane displacement at the critical load (Fine Mesh).

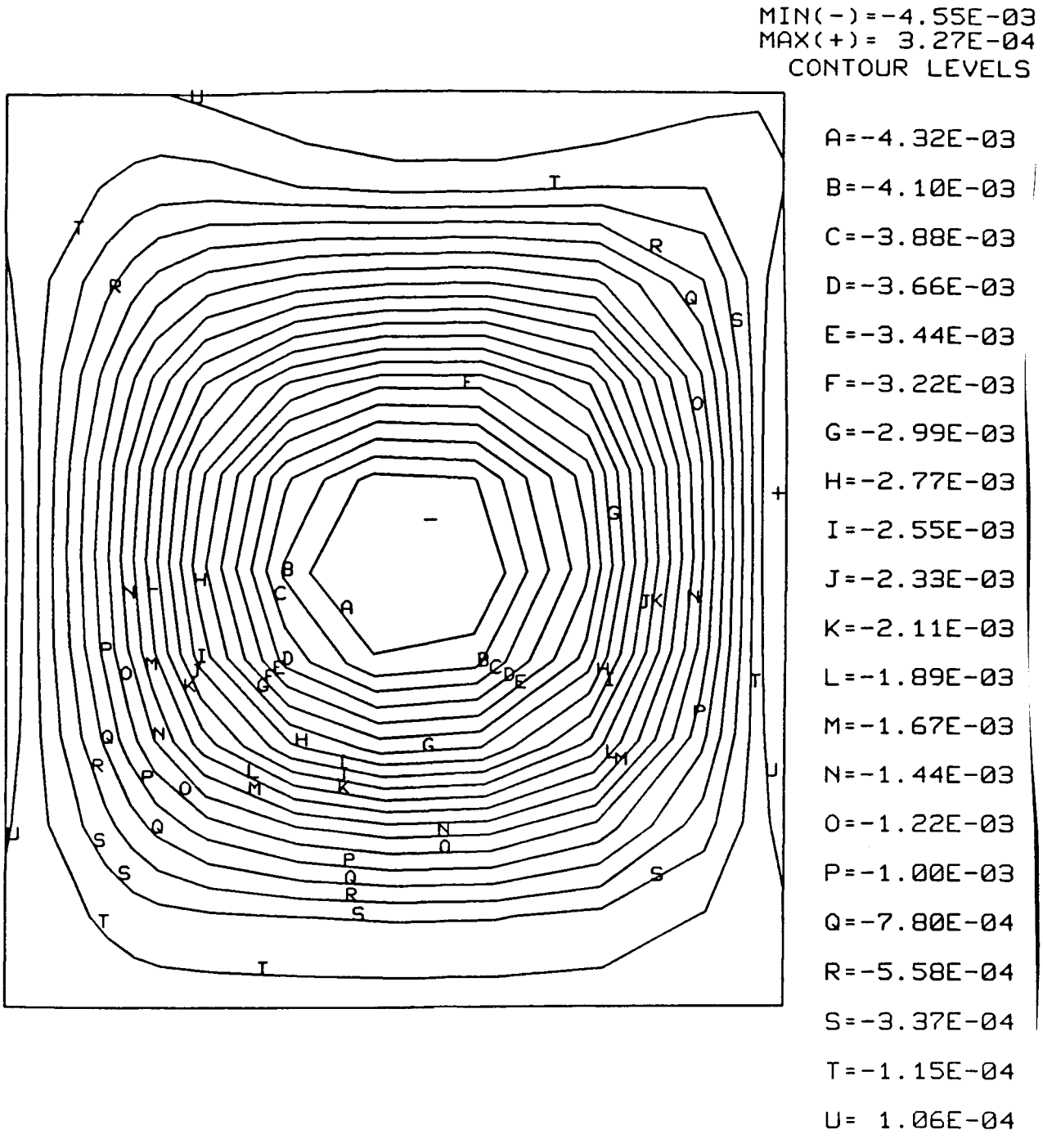

Figure 3b. Contours of constant out-of-plane displacement at the critical load (Coarse Mesh).

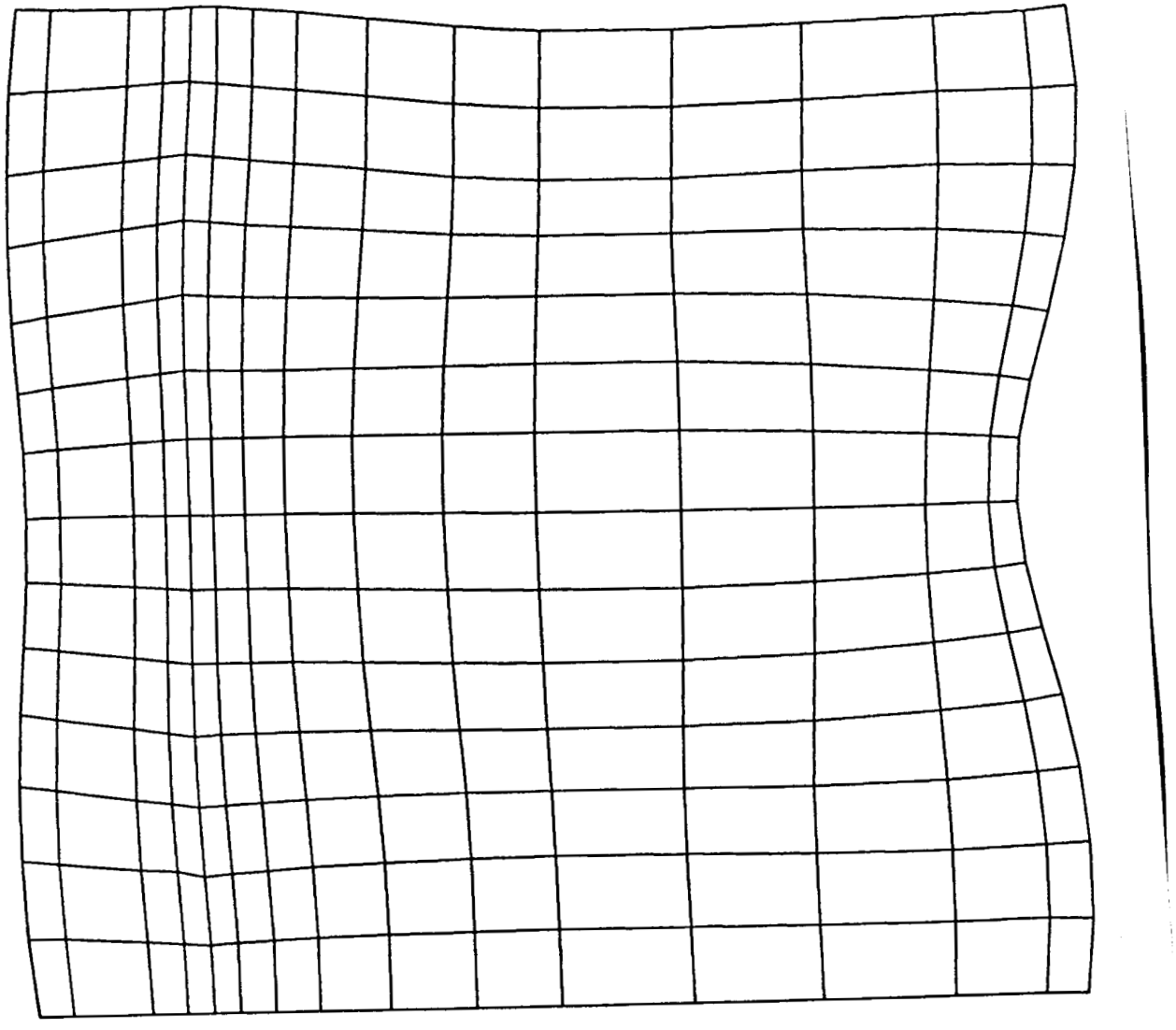

Figure 4a. In-plane Deformation (Fine Mesh).

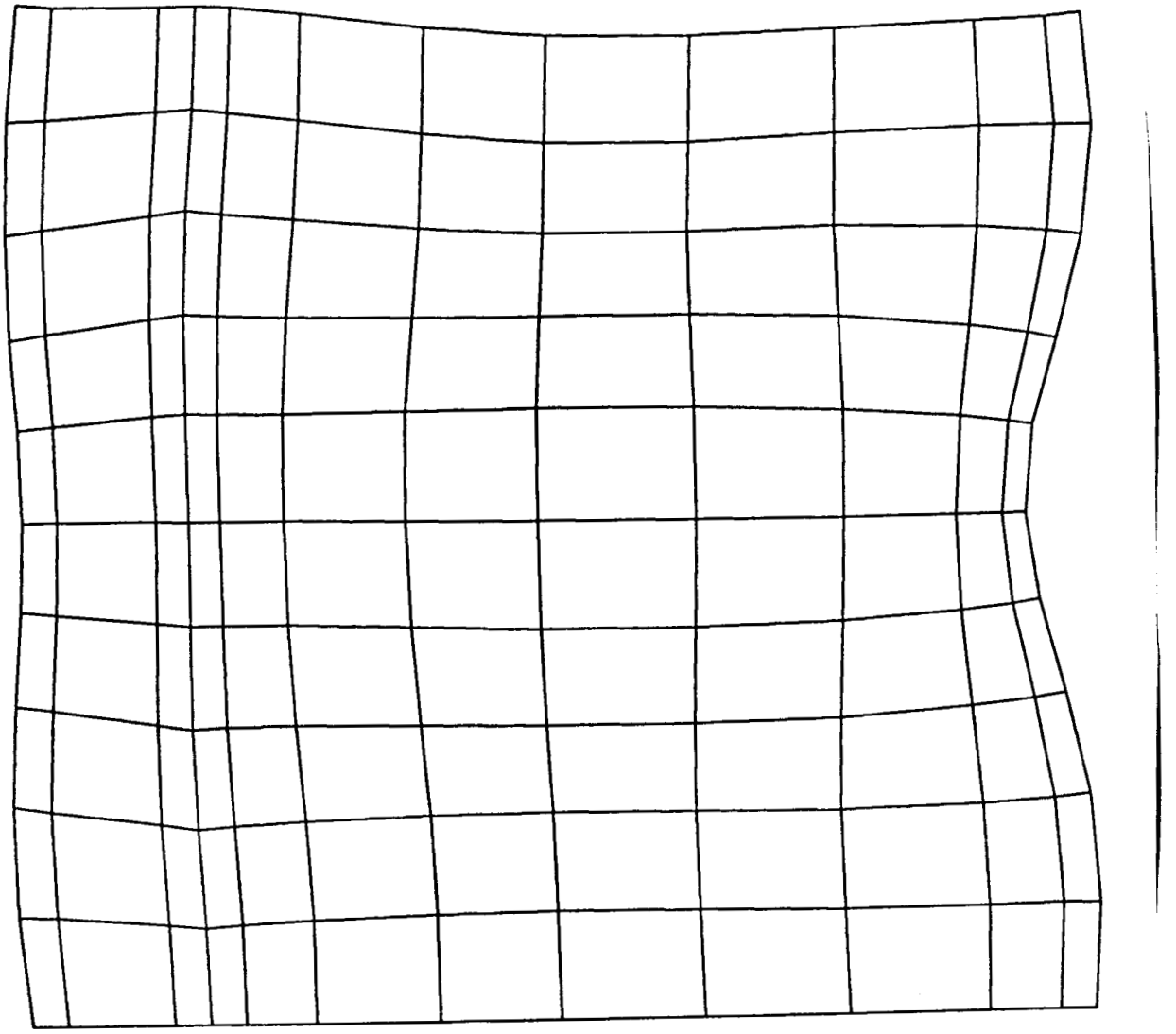

Figure 4b. In-plane Deformation (Coarse Mesh).

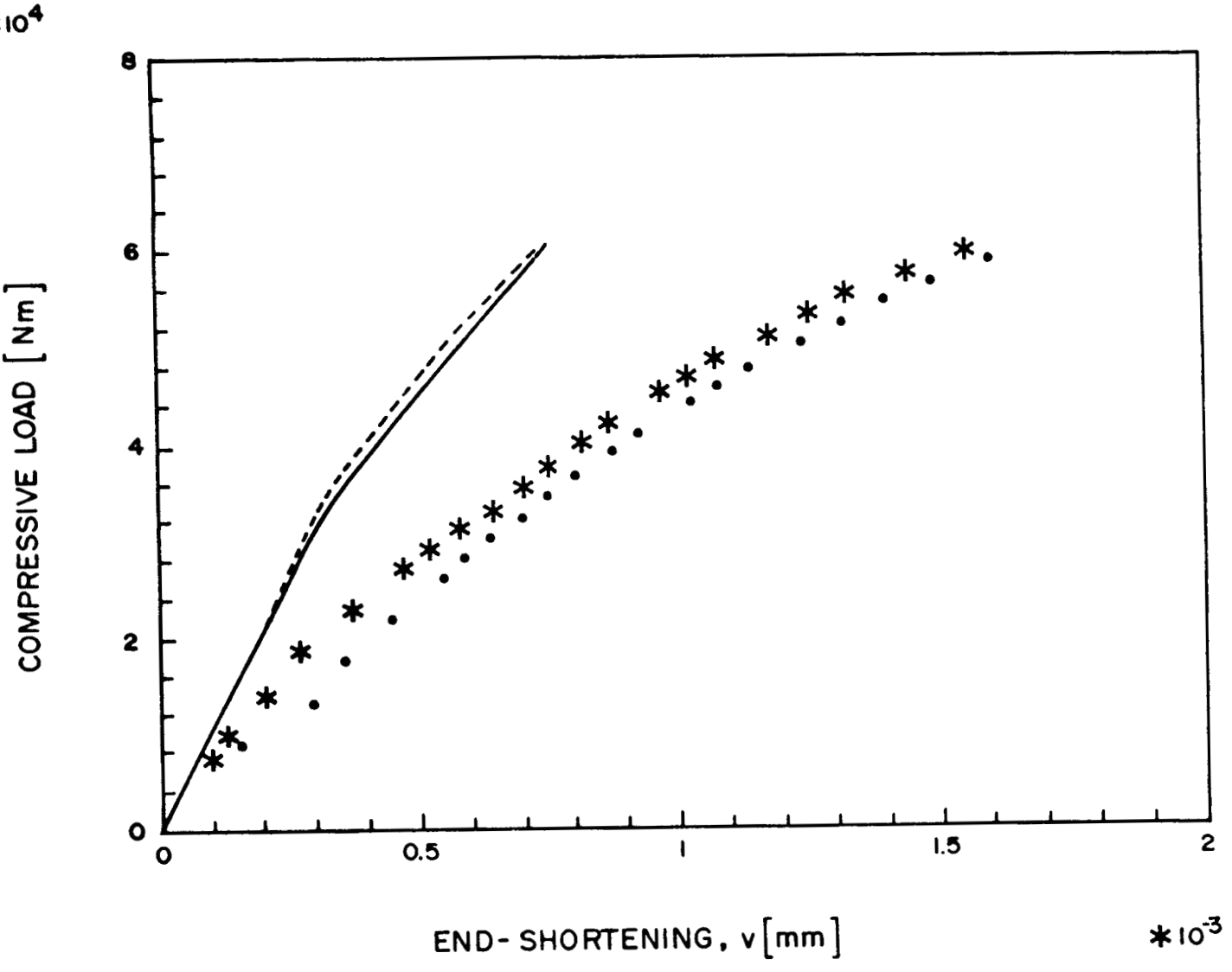

Figure 5. In-plane End Load vs. End-shortening.

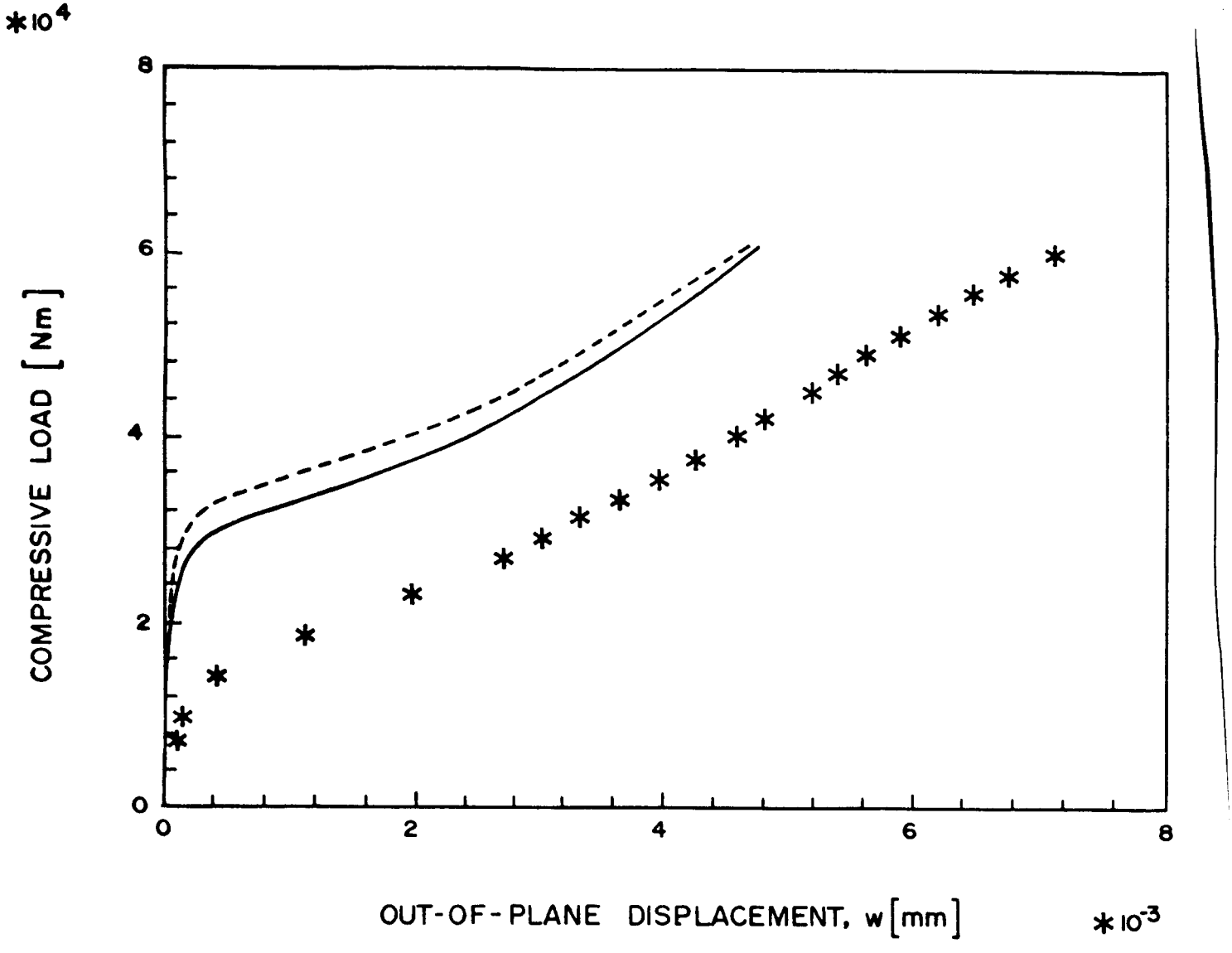

Figure 6. In-plane End Load vs. Out-of-plane Displacement in the middle of the panel.

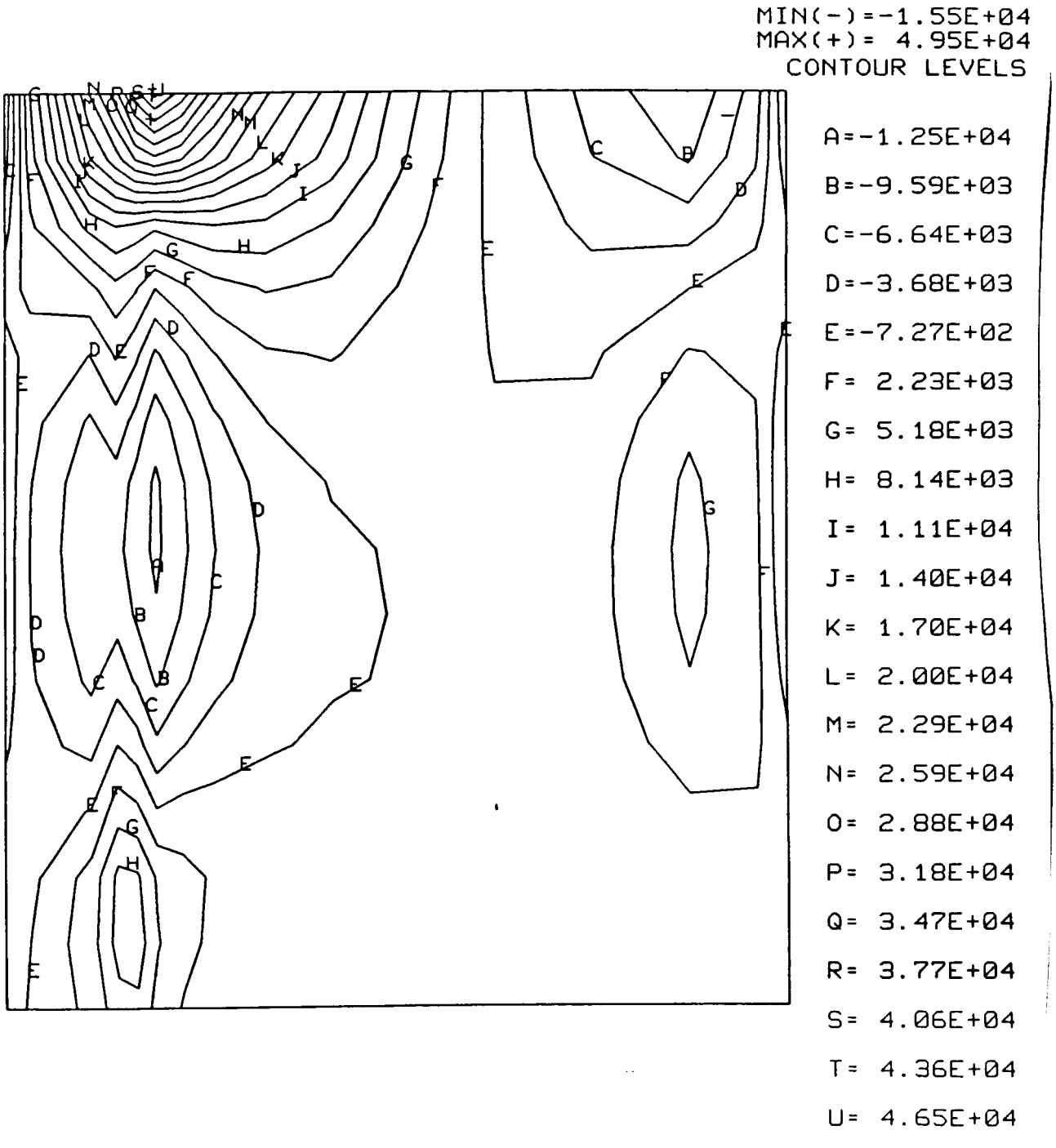

Figure 7a. Contours of constant Shear Force Q_X (Fine Mesh).

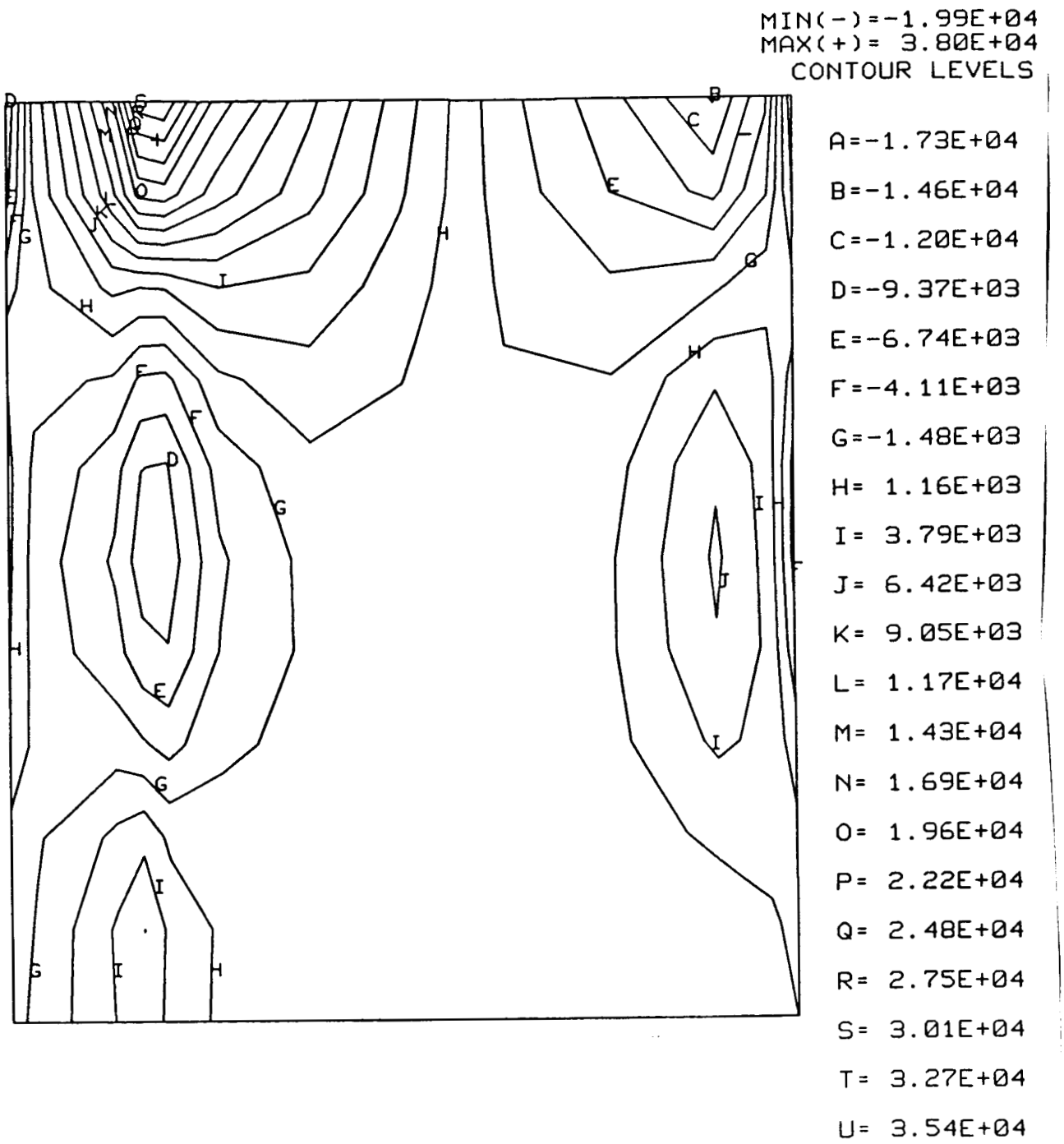

Figure 7b. Contours of constant Shear Force Q_x (Coarse Mesh).